

# SEXTUPOLE MAGNETS FOR DIAMOND

J.A.Clarke and N.Marks, CLRC, Daresbury Laboratory, Warrington WA4 4AD, UK.

## Abstract

The paper presents details of preliminary investigation on the achromat sextupoles for DIAMOND. The pole geometry, which is subject to geometrical constraints, is given and the predicted sextupole field quality presented. The paper then examines the generation of vertical and horizontal dipole correction fields, by the use of auxiliary coils within the sextupole configuration, in more detail and presents solutions which are believed to be a satisfactory basis for further engineering design.

## 1 INTRODUCTION

Work on a possible future synchrotron radiation source DIAMOND is proceeding at the Daresbury Laboratory. The present study is based on a third generation, 3 GeV storage ring light source, with full energy injection from a booster synchrotron. Preliminary investigations on the dipoles and quadrupoles for the storage ring lattice are reported elsewhere [1], whilst this paper presents a summary of present work on the achromat sextupoles. In all cases, the magnetic field distributions shown have been predicted using the Vector Fields code OPERA 2D. It should be appreciated that this work has not been carried out on the scale of a full design study, but rather as a feasibility exercise on which future detailed designs can be based.

## 2 SEXTUPOLE FIELDS

The achromat sextupoles currently have the following magnetic parameters:

max sextupole gradient $g_s$	135 T m <sup>-2</sup> ;
sextupole gradient tolerance	± 1% ;
in range	$0 \leq  x  \leq 35$ mm.

Geometric tolerances imposed by the electron and x-ray beam tube requirements are:

inscribed radius $R_s$	≥ 40 mm ;
minimum allowed vertical pole clearance	± 10 mm.

This latter restraint is to provide adequate clearance for the emerging beams of synchrotron radiation.

Various pole geometries were explored and it was established that, with the constraint on the minimum pole gap, the required gradient tolerance could not be

achieved with an inscribed radius of less than 46mm. Fig 1 shows the quadrant geometry used in OPERA 2D which provided close to the required tolerance. The pole comprises six linear regions which approximate to the theoretical third order curve. It can be seen that the last such linear region at the extremity of the  $\pi/6$  pole is at  $y = 10$ mm and is parallel to the x axis. This was found to be effective in extending the region of useful gradient whilst still meeting the geometric constraints.

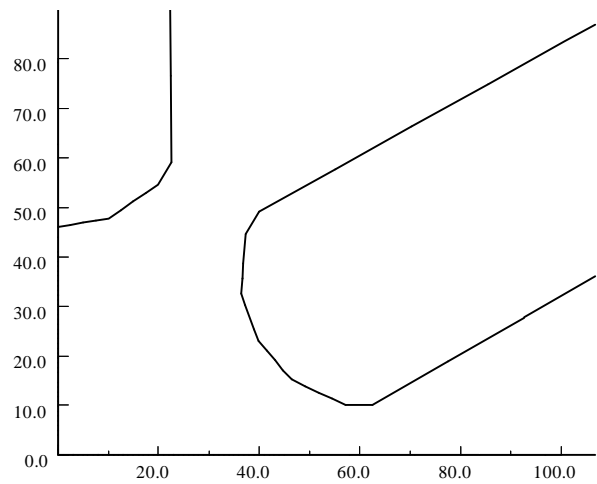


Fig: 1 Geometry used for sextupole gradient modelling (dimensions in mm).

The sextupole gradient quality predicted with linear iron is shown in Fig 2 as the percentage variation of  $d^2B_y / dx^2$  vs  $x$ . It can be seen that the sextupole field quality approaches the specified tolerance, with the gradient being 1% low at approximately  $x = 33$ mm.

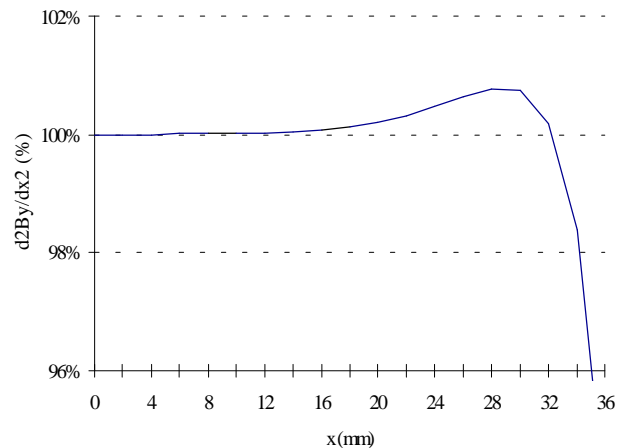


Fig: 2 Sextupole gradient expressed as the percentage variation of  $d^2B_y / dx^2$  vs  $x$ .

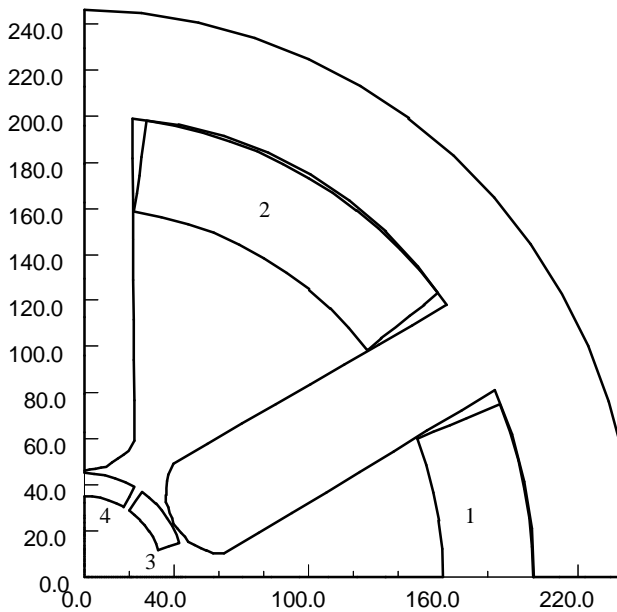


Fig. 3 Steel and coil geometry used for the investigation of the superposition of dipole field in the sextupole magnet (dimensions in mm).

The suitability of this geometry will finally be determined by particle tracking through the lattice, when it will be possible to assess the reduction in dynamic aperture resulting from the sextupole gradient errors.

### 3 DIPOLE CORRECTION FIELDS

Closed orbit adjustment is now an important feature of third generation sources, both to ensure good beam lifetimes and to steer the beam to align emerging radiation. Previous investigations [2] [3] have used a number of exotic geometries to generate dipole correction fields in main lattice magnets. Alternative solutions to this problem were therefore investigated, with the aim of introducing independent, fully adjustable vertical and horizontal dipole correction fields into the sextupole. The following parameters were specified for these dipole correctors:

max. vertical and horizontal field amplitude	0.075 T;
field quality	$\pm 1\%$ ;
horizontal aperture	$0 \leq  x  \leq 30$ mm ;
vertical aperture	$0 \leq  y  \leq 20$ mm.

A number of different coil geometries were examined; the coil combinations for which results are predicted are shown in Fig 3. Two coils are positioned between the poles, close to the backleg, and these are used for generating both vertical and horizontal field. They generate Ampere-turns at the poles, to approximate to the cosine and sine distributions which are required

for the ideal vertical and horizontal field distributions; as the detailed sizes or positions of these coils do not influence the field quality, their shape and position as shown do not correspond to a realistic engineering solution. They are referred to as:

Coil 1	commencing at	$0^\circ$
	terminating at	$22^\circ$
Coil 2	commencing at	$38^\circ$
	terminating at	$82^\circ$

where the angles are measured with respect to the x axis.

Two further, smaller coils are positioned in a cylindrical distribution on the pole face. As the inscribed radius of the magnet is, of necessity, greater than that needed to accommodate the electron beam vacuum vessel, this space is available for the pole-face coils. They can therefore be used to provide the current sheaths which are clearly necessary if good quality dipole fields, which have components that are parallel to the pole faces, are to be established in the beam region. The geometric specification of these two pole-face coils is:

inner radius	35 mm ;	
outer radius	45 mm;	
Coil 3	commences at	$19^\circ$
	terminates at	$55^\circ$
Coil 4	commences at	$60^\circ$
	terminates at	$90^\circ$

The  $5^\circ$  gap between these coils has been included to provide space in the future for a possible water-cooling channel or other necessary engineering features. The quarter magnet geometry of Fig 3, with linear steel, was used throughout the simulation exercises; symmetry conditions, which ensured that the return coils in the hidden quadrants had the correct current polarities, were imposed.

#### 3.1 Vertical Dipole Field

Initial investigations were carried out with just coils 1 and 2 excited. Initially, current densities approximating to a cosine law were used, but better vertical field distributions were obtained with increased current levels in coil 2. The best results were obtained using the following excitation levels:

coil 1	42.5% of total At;
coil 2	57.5% of total At.

The resulting vertical field homogeneity is shown in Fig 4; the field drops to 1% below the central value at  $x = 16$ mm and then rises rapidly, exceeding the allowed tolerance beyond  $x = 24$ mm.

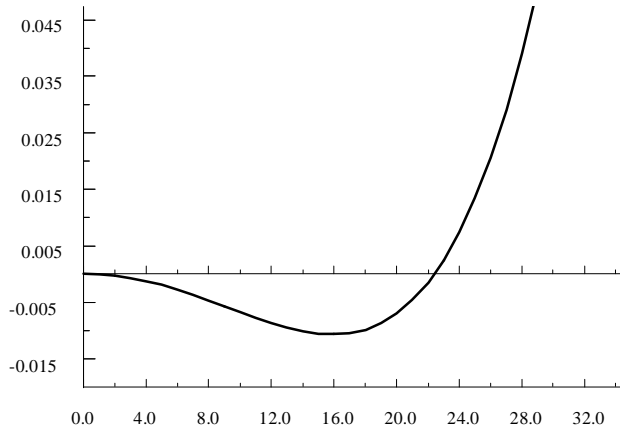


Fig: 4 Fractional homogeneity of vertical dipole field as a function of horizontal position  $x$  (mm) on the  $y = 0$  axis, with coils 1 and 2 excited.

Adding excitation to coil 3 was found to significantly improve this situation. With very high current densities in this coil (of the order of  $8 \text{ A/mm}^2$ ), field distributions better than  $\pm 0.5\%$  out to  $x = 30\text{mm}$  were predicted. However, such current densities in small pole-face windings are not believed to be realistic and would lead to thermal and termination difficulties. Current levels that corresponded to more practical engineering situations were therefore investigated.

Satisfactory results were obtained with a realisable current density, ( $3.5 \text{ A/mm}^2$ ) in coil 3, with good field out to  $x = 29\text{mm}$ . Fig 5 shows the vertical field distribution obtained with the following excitations:

coil 1	38.2% of total $At$ ;
coil 2	38.2% of total $At$ ;
coil 3	23.6% of total $At$ .

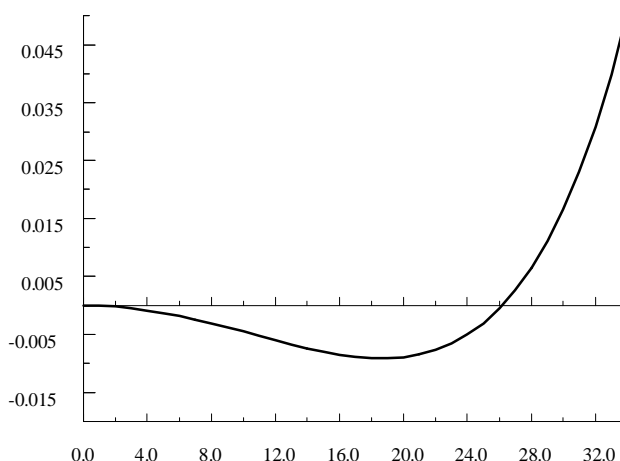


Fig: 5 Fractional homogeneity of vertical dipole field as a function of horizontal position  $x$  (mm) on the  $y = 0$  axis, with coils 1, 2 and 3 excited.

### 3.2 Horizontal Dipole Field.

Horizontal field was first produced from coil 2 alone, with suitable return symmetry; this gave poor horizontal field distribution, which dropped below 99% at  $y = 15\text{mm}$ . The inclusion of current in coil 4 considerably improved the situation. With the following excitations:

coil 2	83.6% of total $At$ ;
coil 4	16.4% of total $At$ ;

the horizontal field distribution shown in Fig 6 was obtained. The field is within  $\pm 1\%$  to  $y = 24\text{mm}$ .

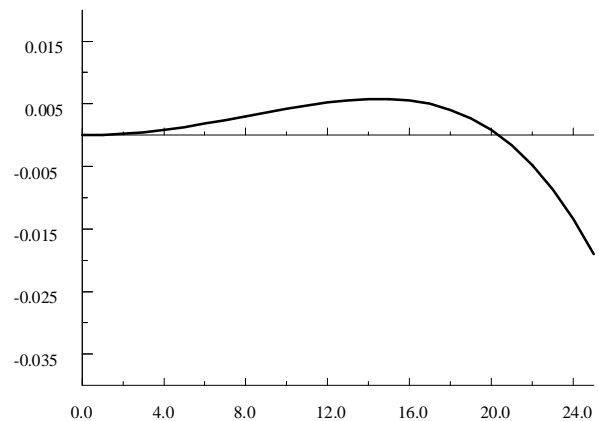


Fig: 6 Homogeneity of horizontal dipole field as a function of vertical position  $y$  (mm) on the  $x = 0$  axis, with coils 2 and 4 excited.

## 4 CONCLUSION

This preliminary work has established methods of producing fully independently adjustable vertical and horizontal dipole fields in the DIAMOND sextupoles magnets. Further investigations are required to establish whether the sextupole gradient and dipole quality are adequate to give good dynamic aperture in the storage ring. This will then need to be followed by a more detailed engineering design that will resolve the practical problems of the magnet.

## REFERENCES

- [1] 'Dipole and Quadrupole Magnet Designs for DIAMOND', N. Bliss, J.A. Clarke, M. Harold and N. Marks, these proceedings.
- [2] 'Combined A.C. Corrector Magnets', N. Marks, A.J. Otter and P.A. Reeve, proc. 1993 Part. Accel. Conf., Washington, D.C.
- [3] 'The SRS Prototype Multipole Magnet', N. Marks, Proc. 6th Int. Mag. Tech. Conference, Bratislava, 1977.